IEEE Access
Multidisciplinary | Rapid Review | Open Access Journal

IEEE POWER & ENERGY SOCIETY SECTION

Received February 12, 2021, accepted February 28, 2021, date of publication March 2, 2021, date of current version March 10, 2021.

Digital Object Identifier 10.1109/ACCESS.2021.3063610

A Hybrid Energy and Mode Decomposition-Based Method for Evaluating Generators Damping in Multi-Machine Power Systems

JIAN XIE[1], (Graduate Student Member, IEEE), WEI SUN[1], (Member, IEEE), KAI SUN[2], (Senior Member, IEEE), AND XIAORU WANG[3], (Senior Member, IEEE)

[1]Department of Electrical and Computer Engineering, University of Central Florida, Orlando, FL 32816, USA
[2]Department of Electrical Engineering and Computer Science, The University of Tennessee, Knoxville, TN 37996, USA
[3]Department of Electrical Engineering, Southwest Jiaotong University, Chengdu 611756, China

Corresponding authors: Jian Xie (jianxie@knights.ucf.edu) and Wei Sun (sun@ucf.edu)

ABSTRACT The increasing number of low-frequency oscillation events has posed significant challenges to power system stability. It is imperative to accurately identify and properly control generators with poor or negative damping contribution for better oscillation damping. This paper proposes a hybrid energy and mode decomposition-based method for evaluating generators damping in multi-machine power systems. It is derived that the aggregate electric torque can be modeled as the superposition of electric torques in different modes. In each oscillation mode, the electric torque can be decomposed into the damping torque and the synchronizing torque. Moreover, a novel oscillation energy function is developed to evaluate generators' damping effect in each oscillation mode. The result proves that in each oscillation mode, generators with attenuated oscillation energies have negative damping effects. Simulation results in single and multinegative damping generators cases, as well as the comparison with other methods, demonstrate the effectiveness and robustness of the proposed method for damping evaluation.

INDEX TERMS Damping torque, low frequency oscillation, multi-machine power systems, oscillation energy, oscillation suppression.

NOMENCLATURE

$\Delta\delta_i, \Delta\omega_i$	Rotor angle and speed of generator i
$\Delta\delta_i\|_{\lambda_r}$	Angle component in r^{th} mode of generator i
$\Delta\omega_i\|_{\lambda_r}$	Speed component in r^{th} mode of generator i
$\Delta\omega_i\|_{\lambda_r,k}$	k^{th} measurement of the speed deviation in mode r of generator i
$\Delta E'_{qi}$	q-axis transient electromotive force of generator i
ΔE_{fdi}	Excitation voltage of generator i
$\Delta P_{ei}\|_{\lambda_r}$	Oscillation component deviation of the electric power in mode r of generator i
ΔT_{ei}	Deviation of the electric torque in generator i
$\Delta T_{ei}\|_{\lambda_r,k}$	k^{th} measurement of the deviation of the electric torque in mode r of generator i
$\Delta T_{ei}\|_{\lambda_r}$	Deviation of the electric torque in mode r of generator i
F	Dot product of electric torque and speed vector
s	Laplace operator
$\mathbf{\Delta\delta}$, $\mathbf{\Delta\omega}$	Rotor angle and speed vector of generators
$\mathbf{\Delta E'}_q$	q-axis transient electromotive force vector
$\mathbf{\Delta E_{fd}}$	q-axis transient electromotive force vector
$\mathbf{\Delta T}_e$	Electric torque deviation vector
$\mathbf{A}$	State matrix
$\mathbf{B}\,(s)$	Electric torque coefficient matrix
$\mathbf{I}$	Identity matrix
$\mathbf{M}$, $\mathbf{D}$	Inertia time constant and mechanical damping matrix of generators
$\mathbf{x}$	State vectors in multi-machine power system
$\mathbf{Z}\,(s)$	A vector
λ_r	Eigenvalue in r^{th} oscillation mode
ω_r	Angular frequency in the r^{th} oscillation mode
σ_r	Attenuation factor in the r^{th} oscillation mode
θ_r	Initial phase in the r^{th} oscillation mode
A_r	Amplitude in the r^{th} oscillation mode

The associate editor coordinating the review of this manuscript and approving it for publication was Guangya Yang.

$B_{ij}(s)$	Coefficient between angles of generator i and j
$K_{di}\|_{\lambda_r}$	Damping torque coefficient in mode r of generator i
$K_{ei}(s)$	Electric torque coefficient in generator i
$K_{si}\|_{\lambda_r}$	Synchronizing torque coefficient in mode r of generator i
$K_{\mathbf{e}i}\|_{s_r}$	Electric torque coefficient in mode r of generator i
M_i, D_i	Inertia and mechanical damping coefficient of generator i
T'_{d0i}	d axis open circuit transient time constant of generator i
W_{ir}	Oscillation energy of generator i for the r^{th} mode
$x_k(t)$	Time response of k^{th} state variable
$z_i(s)$	i^{th} element in $\mathbf{Z}(s)$
α_r	Real part of eigenvalue in mode r
$\mathbf{K}_m$	Coefficient matrices determined by the system operating conditions
$\mathbf{K_e}(s)$	Electric torque coefficient matrix in multi-machine system
$\mathbf{K}_\mathrm{A}$	Matrix of gains of the automatic voltage regulators
$\mathbf{T}_\mathrm{A}$	Matrix of constants of the automatic voltage regulators
$\mathbf{T}_{d0}$	d-axis open circuit transient time constant matrix of generators
Ω_r	Oscillation angular frequency in mode r
$K_{\mathrm{A}i}$	Gain of the automatic voltage regulator in generator i
$P_{ei}\|_{\lambda_r}$	Oscillation component of the electric power in mode r of generator i
$T_{\mathrm{A}i}$	Constant of the automatic voltage regulator in generator i

I. INTRODUCTION

The more frequent low-frequency oscillation events are jeopardizing the normal operation of the power grid, and they may cause a large-scale outage or blackouts [1]–[3]. Especially, the oscillations with poor or even negative damping may pose a serious threat to power system security and deteriorate the power transfer capability. Damping torque has been widely used to evaluate the damping effect of generators during power system oscillation [4]–[6]. According to the negative damping theory, generators with high-gain fast exciters can weaken the damping torque and lead to poorly or negatively damped oscillations. Therefore, it is imperative to evaluate the damping torque of each generator, identify generators with poor or negative damping contribution during oscillation, and properly control these generators to damp the oscillations [7], [8].

In the literature, the methods for evaluating oscillation damping provided by generators can be divided into damping torque-based and energy-based methods [9]. First, for damping torque-based methods, authors in [10] estimate the damping and synchronizing torque of generators in a single-machine-infinite-bus (SMIB) system, based on the ordinary least square (OLS) method. A numerical method is then applied to a multi-machine power system assuming the damping torque of a generator only depends on its own speed deviation [11]. Furthermore, the study in [12] shows that the expression of damping torque in [11] is only valid when the speed deviations for all other generators are zeros. In general, the damping torque of each rotor depends on the speed deviation of other rotors [12]. In [13], authors adopt the OLS method and the mode decomposition technique to calculate damping coefficients in the dominant oscillation mode. However, the prerequisite of this method is that there exists only one dominant oscillation mode in power systems, which significantly limit the application in practice. In [6] , an oscillation phasor concept is proposed to identity generator with poor damping effect, and a two-step method based on phasor and energy analysis is proposed to evaluate generators' damping in [14].

Next, for transient energy-based methods, authors in [7] propose an energy-based method to evaluate the damping effects of generators. However, it needs further investigation to prove the applicability of the single-mode oscillation approach in multi-machine power systems [7]. This energy-based method has been further developed in [8], [15], [16]. In [8], the original energy-based method is improved to a more robust Dissipating Energy Flow (DEF) method. In [17], the energy-based method is extended to evaluate the damping effect of a prime mover, but an accurate mechanical power is difficult to obtain in order to implement that method. The consistency of energy dissipation with damping torque has been proved in the Heffron-Phillips model in the SMIB system. In [18], the transient energy is transformed into a frequency domain to estimate damping torque coefficients and evaluate each component's damping during ambient conditions. The energy function is represented as the integral of the product of generator's measurements. However, in actual power systems, the measurement data usually contain noises, and the calculation of energy flow using raw measurements may not guarantee accurate results. In addition, in order to obtain a robust result by the method proposed in [8], the duration of time interval should contain 20 to 40 periods of oscillations, about 28s to 400s, which is slow for online analysis. Therefore, it is necessary to develop methods to effectively and fast evaluate the damping effects of generators and locate generators that bring negative damping in multi-machine power systems.

To address the aforementioned challenges and find a more efficient way to evaluate generators' damping effects during a oscillation process, this paper proposes a hybrid energy and mode decomposition-based approach to evaluate generators damping in multi-machine power systems. The main contributions of this paper are three-fold: 1) based on the mathematical derivation, the damping torque of each generator in multi-machine power systems is analyzed and expressed as the superposition of electric torques in different modes; 2) a novel and simple oscillation energy function is defined and

then aggregated with the mode decomposition to evaluate the damping effect of each generator in each oscillation mode; 3) with a mode decomposition process, the raw measurements are decomposed into several noise-free oscillation components, which are utilized to calculate the oscillation energies; thus, the proposed method is robust to measurement noises.

The rest of the paper is structured as follows. Section II studies the damping torque of each generator in multi-machine power systems. Section III presents a novel oscillation energy function. In section IV, a step-by-step process is presented to evaluate damping provided by each generator in multi-machine power systems. In section V, the proposed method is verified and compared with other methods in multiple test cases. Finally, section VI concludes this paper.

II. DAMPING TORQUES DERIVATION OF MULTI-MACHINE POWER SYSTEMS

In this section, the expression of electric torque of each generator is derived and decomposed based on the Heffron-Phillips model of multi-machine power systems. The linearized model of a multi-machine system is introduced first, and then the electric torque in the multi-machine system is derived and decomposed into damping and synchronizing torques in different oscillation modes.

A. LINEARIZED MODEL

According to [19], power system oscillations can be viewed as a small-signal stability problem, and the linearized model of an n-machine power system can be represented as follows,

$$\begin{bmatrix} \Delta\dot{\boldsymbol{\delta}} \\ \Delta\dot{\boldsymbol{\omega}} \\ \Delta\dot{\mathbf{E}}'_{\mathbf{q}} \\ \Delta\dot{\mathbf{E}}_{\mathbf{fd}} \end{bmatrix} = \mathbf{A} \begin{bmatrix} \Delta\boldsymbol{\delta} \\ \Delta\boldsymbol{\omega} \\ \Delta\mathbf{E}'_{\mathbf{q}} \\ \Delta\mathbf{E}_{\mathbf{fd}} \end{bmatrix} \tag{1}$$

where

$$\begin{aligned} \Delta\boldsymbol{\delta} &= \begin{bmatrix} \Delta\delta_1 & \Delta\delta_2 & \cdots & \Delta\delta_n \end{bmatrix}^{\mathrm{T}} \\ \Delta\boldsymbol{\omega} &= \begin{bmatrix} \Delta\omega_1 & \Delta\omega_2 & \cdots & \Delta\omega_n \end{bmatrix}^{\mathrm{T}} \\ \Delta\mathbf{E}'_q &= \begin{bmatrix} \Delta E'_{q1} & \Delta E'_{q2} & \cdots & \Delta E'_{qn} \end{bmatrix}^{\mathrm{T}} \\ \Delta\mathbf{E}_{\mathbf{fd}} &= \begin{bmatrix} \Delta E_{fd1} & \Delta E_{fd2} & \cdots & \Delta E_{fdn} \end{bmatrix}^{\mathrm{T}} \\ \mathbf{M} &= diag\left(M_i\right), \mathbf{D} = diag\left(D_i\right), \quad \mathbf{T}_{d0} = diag\left(T'_{d0i}\right) \\ \mathbf{K}_{\mathrm{A}} &= diag\left(K_{\mathrm{A}i}\right), \quad \mathbf{T}_{\mathrm{A}} = diag\left(T_{\mathrm{A}i}\right) \end{aligned}$$

$\mathbf{K_1}, \mathbf{K}_2, \mathbf{K}_3, \mathbf{K}_4, \mathbf{K}_5 \in R^{n\times n}$ are coefficient matrices determined by system operating conditions. Subscript i represents variables associated with i^{th} machine, and $diag(a_i)$ denotes the n-order diagonal matrix with i^{th} element as a_i. $\mathbf{A}$ is the state matrix:

$$\mathbf{A} = \begin{bmatrix} \mathbf{0} & \boldsymbol{\omega_0}\mathbf{I} & \mathbf{0} & \mathbf{0} \\ -\mathbf{M}^{-1}\mathbf{K_1} & -\mathbf{M}^{-1}\mathbf{D} & -\mathbf{M}^{-1}\mathbf{K_2} & \mathbf{0} \\ -\mathbf{T}_{\mathbf{d0}}^{-1}\mathbf{K_4} & \mathbf{0} & -\mathbf{T}_{\mathbf{d0}}^{-1}\mathbf{K_3} & -\mathbf{T}_{\mathbf{d0}}^{-1} \\ -\mathbf{T}_{\mathbf{A}}^{-1}\mathbf{K_5}\mathbf{K_A} & \mathbf{0} & -\mathbf{T}_{\mathbf{A}}^{-1}\mathbf{K_5}\mathbf{K_A} & -\mathbf{T}_{\mathbf{A}}^{-1} \end{bmatrix}$$

Equation (1) is the Heffron-Phillips model of a multi-machine power system [19], as shown in Fig. 1. Equation (1) can be represented as follows,

$$\dot{\mathbf{x}} = \mathbf{A}\mathbf{x} \tag{2}$$

where $\mathbf{x} = \begin{bmatrix} \boldsymbol{\Delta\delta} & \boldsymbol{\Delta\omega} & \mathbf{\Delta E'_q} & \mathbf{\Delta E_{FD}} \end{bmatrix}$.

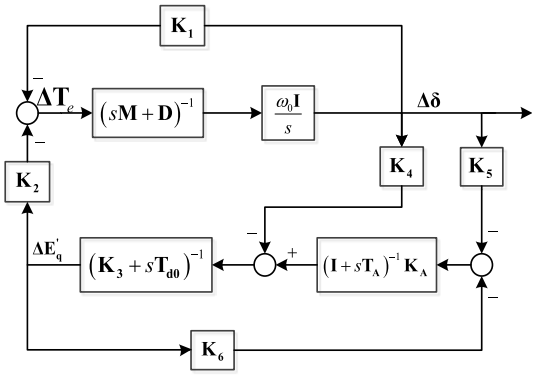

FIGURE 1. Heffron-Phillips model of an n-machine power system.

Based on [20], for an n-machine power system as described by equation (1) or Fig. 1, $\mathbf{\Delta T}_e$ and $\mathbf{\Delta E'}_q$ have the following relationship, with s as the Laplace operator:

$$\mathbf{\Delta T}_e = \mathbf{K}_1\boldsymbol{\Delta\delta} + \mathbf{K}_2\mathbf{\Delta E'}_q \tag{3}$$

$$\begin{aligned} \mathbf{\Delta E'}_q &= \left(\mathbf{T'_{d0}}s + \mathbf{K}_3 + (\mathbf{T}_{\mathrm{A}}s + \mathbf{I})^{-1}\mathbf{K}_{\mathrm{A}}\mathbf{K}_6\right)^{-1} \\ &\quad \cdot \left(-\mathbf{K}_4 - (\mathbf{T}_{\mathrm{A}}s + \mathbf{I})^{-1}\mathbf{K}_{\mathrm{A}}\mathbf{K}_5\right)\boldsymbol{\Delta\delta} \\ &= \mathbf{H}\left(s\right)\boldsymbol{\Delta\delta} \end{aligned} \tag{4}$$

B. DERIVATION OF ELECTRIC TORQUES IN MULTI-MACHINE SYSTEMS

Substitute equation (3) into (4) to obtain the following,

$$\mathbf{\Delta T_e} = \mathbf{B}\left(\mathbf{s}\right)\boldsymbol{\Delta\delta} \tag{5}$$

where $\mathbf{B}\left(s\right)$ is the electric torque coefficient matrix:

$$\mathbf{B}\left(s\right) = \begin{bmatrix} B_{11}\left(s\right) & B_{12}\left(s\right) & \cdots & B_{1n}\left(s\right) \\ B_{21}\left(s\right) & B_{22}\left(s\right) & \cdots & B_{2n}\left(s\right) \\ \vdots & \vdots & \ddots & \vdots \\ B_{n1}\left(s\right) & B_{n2}\left(s\right) & \cdots & B_{nn}\left(s\right) \end{bmatrix}$$

In addition, the relationship between $\mathbf{\Delta T_e}$ and $\boldsymbol{\Delta\omega}$ can be derived from equation (1) as follows,

$$\begin{aligned} s\boldsymbol{\Delta\omega} &= -\mathbf{M}^{-1}\left(\mathbf{K}_1\boldsymbol{\Delta\delta} + \mathbf{K}_2\mathbf{\Delta E'}_q + \mathbf{D}\Delta\omega\right) \\ &= -\mathbf{M}^{-1}\left(\mathbf{\Delta T}_e + \mathbf{D}\Delta\omega\right) \end{aligned} \tag{6}$$

Set $\mathbf{D} = \mathbf{0}$ and combine (1) and (6) to obtain the following,

$$\mathbf{\Delta T_e} = -\frac{\mathbf{M}s^2}{\boldsymbol{\omega}_0}\boldsymbol{\Delta\delta} \tag{7}$$

Considering $\omega_0 = 1$ and combining (5) and (7):

$$\begin{bmatrix} B_{11}(s) & B_{12}(s) & \cdots & B_{1n}(s) \\ B_{21}(s) & B_{22}(s) & \cdots & B_{2n}(s) \\ \vdots & \vdots & \ddots & \vdots \\ B_{n1}(s) & B_{n2}(s) & \cdots & B_{nn}(s) \end{bmatrix} \boldsymbol{\Delta\delta} = -\mathbf{M}s^2\boldsymbol{\Delta\delta} \quad (8)$$

where $\boldsymbol{\Delta\delta} = \begin{bmatrix} \Delta\delta_1 & \Delta\delta_2 & \cdots & \Delta\delta_n \end{bmatrix}^{\mathrm{T}}$.

Let

$$\mathbf{MM} = \begin{bmatrix} M_2s^2 & 0 & \cdots & 0 \\ 0 & M_3s^2 & & 0 \\ \vdots & & \ddots & 0 \\ 0 & 0 & & M_ns^2 \end{bmatrix}$$

$$\mathbf{BB}(s) = \begin{bmatrix} B_{22}(s) & B_{23}(s) & \cdots & B_{2n}(s) \\ B_{32}(s) & B_{33}(s) & \cdots & B_{3n}(s) \\ \vdots & \vdots & \ddots & \vdots \\ B_{n1}(s) & B_{n2}(s) & \cdots & B_{nn}(s) \end{bmatrix}$$

$$\mathbf{MB} = \mathbf{MM} + \mathbf{BB}$$

If the rotor angle of i^{th} generator $\Delta\delta_i$ is unknown, without loss of generality, assume $i = 1$ and then equation (8) can be rewritten as:

$$\mathbf{MB} \times \begin{bmatrix} \Delta\delta_2 \\ \Delta\delta_3 \\ \vdots \\ \Delta\delta_n \end{bmatrix} = \begin{bmatrix} B_{21}(s) \\ B_{31}(s) \\ \vdots \\ B_{n1}(s) \end{bmatrix} \cdot \Delta\delta_1 \quad (9)$$

Rearrange equation (9) to obtain the following,

$$\mathbf{MB}^{-1} \times \begin{bmatrix} -B_{21}(s) \\ -B_{31}(s) \\ \vdots \\ -B_{n1}(s) \end{bmatrix} \Delta\delta_1 \overset{def}{=} \mathbf{Z}(s)\,\Delta\delta = \begin{bmatrix} \Delta\delta_2 \\ \Delta\delta_3 \\ \vdots \\ \Delta\delta_n \end{bmatrix} \quad (10)$$

where $\mathbf{Z} = \begin{bmatrix} z_2(s) & z_3(s) & \cdots & z_n(s) \end{bmatrix}^{\mathrm{T}}$.

Equation (10) shows that the rotor angle $\Delta\delta_k$ $(k \neq i)$ can be expressed as the function of $\Delta\delta_i$.

Substitute equation (10) into (5) to obtain the following,

$$\begin{aligned} \boldsymbol{\Delta T_e} &= \mathbf{B}(s)\,\boldsymbol{\Delta\delta} \\ &= \mathbf{B}(s) \begin{bmatrix} 1 \\ \mathbf{Z}(s) \end{bmatrix} \Delta\delta_i \\ &= \mathbf{K_e}(s)\,\Delta\delta_i \end{aligned} \quad (11)$$

where $\mathbf{K_e}(s) = \begin{bmatrix} K_{e1}(s) & K_{e2}(s) & \cdots & K_{en}(s) \end{bmatrix}^{\mathrm{T}}$.

Thus, for the i^{th} generator, the deviation of electric torque ΔT_{ei} can be expressed as:

$$\Delta T_{ei} = K_{ei}(s)\,\Delta\delta_i \quad (12)$$

C. TORQUES DECOMPOSITION

Assuming the corresponding eigenvalue to the r^{th} oscillation mode is $\lambda_r = \alpha_r + j\Omega_r$, and denoting $s_r = \lambda_r$, the following equation can be obtained:

$$K_{\mathbf{e}i}|_{\lambda_r} = K_{ei,s}|_{\lambda_r} + j\Omega_r K_{ei,d}|_{\lambda_r} \quad (13)$$

Substitute equation (12) into (13) and consider $\Delta\omega_i|_{\lambda_r} = s_r\Delta\delta_i|_{\lambda_r} = (\alpha_r + j\Omega_r)\,\Delta\delta_i|_{\lambda_r}$ to obtain the following,

$$\begin{aligned} \Delta T_{ei}|_{\lambda_r} &= \left(K_{ei,s}|_{\lambda_r} + j\Omega_r K_{ei,d}|_{\lambda_r}\right)\Delta\delta_i|_{\lambda_r} \\ &= K_{ei,s}|_{\lambda_r}\Delta\delta_i|_{\lambda_r} + j\Omega_r\Delta\delta_i|_{\lambda_r}K_{ei,d}|_{\lambda_r} \\ &\approx K_{si}|_{\lambda_r}\Delta\delta_i|_{\lambda_r} + K_{di}|_{\lambda_r}\Delta\omega_i|_{\lambda_r} \end{aligned} \quad (14)$$

Equation (14) indicates that the electric torque of the i^{th} machine can be decomposed into synchronizing torque and damping torque in a certain oscillation mode, which is similar to the SMIB power system. However, the damping torque coefficient of the i^{th} machine is not constant in multi-machine power systems, which is different from the SMIB power system. The damping torque analysis for SMIB system can be found in [19].

According to the small-signal stability theory, time-domain response of k^{th} state variable of a system is as follows [21]:

$$x_k(t) = \sum_{r=1}^{n-1} A_r e^{j\theta_r} e^{(\sigma_r + j\omega_r)t} = \sum_{r=1}^{n-1} x_k|_{\lambda_r} \quad (15)$$

where λ_r is the eigenvalue of matrix $\mathbf{A}$, A_r is the amplitude, θ_r is the initial phase, σ_r is the attenuation factor, and ω_r is the angular frequency.

Then $\Delta\delta_i$ and $\Delta\omega_i$ can be expressed as follows,

$$\begin{cases} \Delta\delta_i = \sum_{r=1}^{n-1} \Delta\delta_i|_{\lambda_r} \\ \Delta\omega_i = \sum_{r=1}^{n-1} \Delta\omega_i|_{\lambda_r} \end{cases} \quad (16)$$

Substitute equation (16) into (14) to obtain the following,

$$\begin{aligned} \Delta T_{ei} &= K_{ei}(s)\,\Delta\delta_i \\ &= \sum_{r=1}^{n-1} \left[K_{si}|_{\lambda_r}\Delta\delta_i|_{\lambda_r} + K_{di}|_{\lambda_r}\Delta\omega_i|_{\lambda_r}\right] \\ &= \sum_{r=1}^{n-1} K_{ei}|_{\lambda_r}\Delta\delta_i|_{\lambda_r} \end{aligned} \quad (17)$$

Equation (17) shows that the damping torque coefficient and the synchronizing torque coefficient are not constant, but they are formed by the superposition of damping torque and synchronizing torque coefficients in different modes.

III. TORQUES DECOMPOSITION-BASED DEFINITION OF OSCILLATION ENERGY

In this section, an oscillation energy function based on the torque decomposition is presented. The oscillation energy can be computed from wide area monitoring systems data. It will be shown that the oscillation energy can be used to evaluate the damping effect of each generator in different modes.

Based on the above analysis, it is obvious that in each mode, the electric torque can be decomposed into the damping torque and synchronizing torque. Therefore, the coefficients of synchronizing torque and damping torque for mode

r can be expressed as:

$$\Delta T_{ei}|_{\lambda_r} = K_{si}|_{\lambda_r}\Delta\delta_i|_{\lambda_r} + K_{di}|_{\lambda_r}\Delta\omega_i|_{\lambda_r} \tag{18}$$

Combining equations (11) and (18), we can obtain the phase relation of $\Delta T_{ei}|_{\lambda_r}$ and $\Delta\omega_i|_{\lambda_r}$, as shown in Fig. 2.

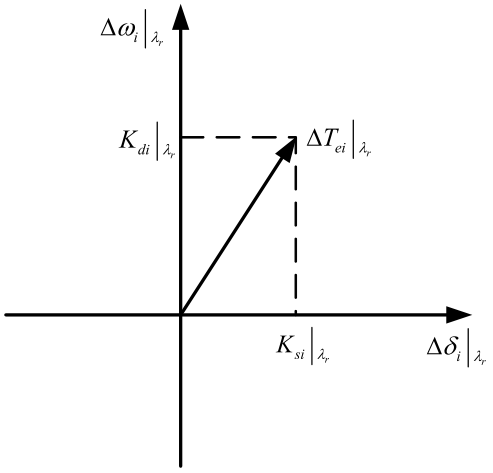

FIGURE 2. Phase relation between $\Delta T_{ei}|_{\lambda_r}$ and $\Delta\omega_i|_{\lambda_r}$.

It is clear the damping torque coefficient $K_{di}|_{\lambda_r}$ is the vector projection of $\Delta T_{ei}|_{\lambda_r}$ onto $\Delta\omega_i|_{\lambda_r}$. If the phase difference of $\Delta T_{ei}|_{\lambda_r}$ and $\Delta\omega_i|_{\lambda_r}$ is between 0° and 90°, $K_{di}|_{\lambda_r}$ will be positive; otherwise, $K_{di}|_{\lambda_r}$ will be negative, and the i^{th} generator has a negative contribution to the damping of the r^{th} oscillation mode.

Assuming that there are L different samples for each state variable, typically several cycles of the dominating mode and the oscillation component can be expressed as:

$$\begin{aligned}\mathbf{\Delta T}_{ei}|_{\lambda_r} &= \begin{bmatrix}\Delta T_{ei}|_{\lambda_r,1} & \Delta T_{ei}|_{\lambda_r,2} & \cdots & \Delta T_{ei}|_{\lambda_r,L}\end{bmatrix}\\ \mathbf{\Delta\omega}_i|_{\lambda_r} &= \begin{bmatrix}\Delta\omega_i|_{\lambda_r,1} & \Delta\omega_i|_{\lambda_r,2} & \cdots & \Delta\omega_i|_{\lambda_r,L}\end{bmatrix}\end{aligned}$$

The dot product of these two vectors can measure their phase difference, which can be expressed as:

$$F = \sum_{j=1}^{L}\Delta T_{ei}|_{\lambda_r,j}\Delta\omega_i|_{\lambda_r,j} \tag{19}$$

From Fig. 2 and Equation (19), we can see that if the dot product $F > 0$, $K_{di}|_{\lambda_r}$ will be positive; otherwise, $K_{di}|_{\lambda_r}$ will be negative, and the i^{th} generator has a negative contribution to the damping of the r^{th} oscillation mode.

Then we can define the oscillation energy of generator i for the r^{th} mode as:

$$\begin{aligned}W_{ir} &= \frac{1}{|c|}\int_c \mathbf{\Delta T}_{ei}|_{\lambda_r} d\,\mathbf{\Delta\delta}_i|_{\lambda_r}\\ &\approx \frac{1}{|c|}\int_c \mathbf{\Delta P}_{ei}|_{\lambda_r} d\,\mathbf{\Delta\delta}_i|_{\lambda_r}\\ &= \frac{1}{t_L - t_1}\int_{t_1}^{t_L}\mathbf{\Delta P}_{ei}|_{\lambda_r}\mathbf{\Delta\omega}_i|_{\lambda_r} dt\end{aligned} \tag{20}$$

where $\mathbf{\Delta P}_{ei}|_{\lambda_r} = \begin{bmatrix}\Delta P_{ei}|_{\lambda_r,1} & \cdots & \Delta P_{ei}|_{\lambda_r,L}\end{bmatrix}$, the subscript c represents the post-disturbance system trajectory "c" regarding this mode, and $\Delta P_{ei}|_{\lambda_r,t}$ denotes the active power deviation at time t of the i^{th} generator in mode λ.

Also, based on the definition of definite integral, we can derive that:

$$\begin{aligned}W &= \frac{1}{t_L - t_1}\int_{t_1}^{t_L}\mathbf{\Delta P}_{ei}|_{\lambda_r}\mathbf{\Delta\omega}_i|_{\lambda_r} dt\\ &\approx \Delta T_{ei}|_{\lambda_r,1}\Delta\omega_i|_{\lambda_r,1} + \cdots + \Delta T_{ei}|_{\lambda_r,L}\Delta\omega_i|_{\lambda_r,L}\\ &= F\end{aligned} \tag{21}$$

Equation (21) proves that the proposed oscillation energy is equivalent to the dot product of electric torque vector and speed vector in (19).

Thus, the novel energy function derived from the torques decomposition in a multi-machine power system can be used to evaluate the damping effect of generators in each mode. In mode r, if the oscillation energy of the i^{th} generator increases with time, the i^{th} generator has a positive damping effect; otherwise, the i^{th} generator has a negative damping effect. Compared with other energy-based methods, the proposed oscillation energy function is proved based on multi-machine power systems and is easier to implement for online analysis.

IV. FLOWCHART OF THE PROPOSED GENERATORS DAMPING EVALUATION METHOD

In this section, the step-by-step implementation of the hybrid energy and mode decomposition-based method is presented for evaluating damping of generators in multi-machine power systems.

From the definition of equation (20), the prerequisite to calculate the oscillation energy is to obtain oscillation parameters such as attenuation factor and frequencies in different oscillation modes. In real power systems, the power system states can be measured by PMU, and then the state deviations can be calculated easily based on the PMU measurements.

Based on [22], these parameters can be estimated from measured signals by modal analysis methods, which means $\Delta T_{ei}|_{\lambda_r}$, $\Delta\omega_i|_{\lambda_r}$ and $\Delta\delta_i|_{\lambda_r}$ can be decomposed from ΔT_{ei}, $\Delta\omega_i$ and $\Delta\delta_i$. Among these modal analysis methods, the Poly-reference Complex Exponential (PRCE) [22] method is fast and robust to measurement noise. The method constructed the auto-regressive model (AR model) from the pulse sequence, using LQ decomposition to solve the self-regression coefficients, and then solved by the roots from polynomial regression coefficient matrix obtained constituting the frequency and damping ratio. Therefore, in this paper, we select the PRCE method to decompose $\Delta T_{ei}|_{\lambda_r}$, $\Delta\omega_i|_{\lambda_r}$ and $\Delta\delta_i|_{\lambda_r}$. Details of the PRCE method for damped signals can be referred in [22].

The flowchart of locating generators with negative damping is shown in Fig. 3, which includes four main steps:

1) Pre-process the input signals and obtain the deviations of active power and speed of all generators;

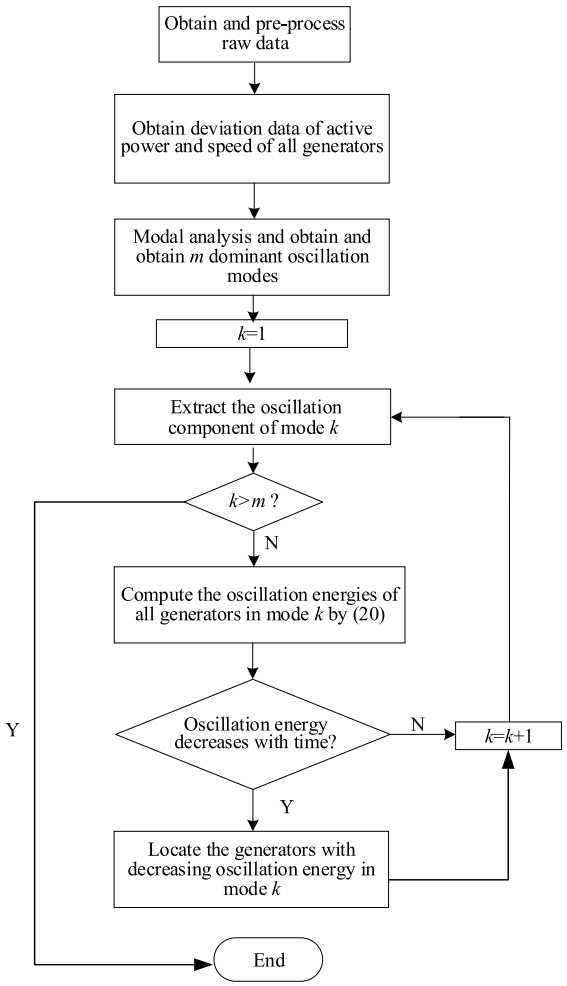

FIGURE 3. Flowchart of locating generators with negative damping.

2) Apply the modal analysis method to obtain the m dominant oscillation modes, and estimate the oscillation parameters of dominant oscillation modes.

3) For the k^{th} $(k = 1, 2, \cdots m)$ mode, reconstruct the k^{th} oscillation component of $\Delta P_{ei}|_{\lambda_k}$ and $\Delta\omega_i|_{\lambda_k}$ by (15);

4) Set $k = 1$, compute the oscillation energy of each generator during mode r by (20), and determine whether there is a negative damping generator for mode k. If not, increase k and go to step 3; otherwise, pinpoint the negative damping generator of mode k, and increase k to continue iteration until satisfying the stopping criterion.

V. SIMULATION RESULTS

The proposed method is tested on three systems, including a four-machine two-area system, a 16-machine system and a Western Electricity Coordinating Council(WECC) 179-Bus system. It should be noted that without loss of generality, a simplified model having a one-axis generator plus a first-order exciter is considered in (1). Conclusions from Section II can be easily extended to more detailed models. Later in the case study, the proposed method is tested on a two-area system with a more detailed two-axis generator model.

A. FOUR-MACHINE TWO-AREA SYSTEM

The system includes four generators, 11 nodes and 12 lines, and it is divided into two areas [23]. In time-domain simulations, generators are described as a detailed two-axis synchronous machine model with static exciter and PSS. The modal damping is also a function of designed PSS parameters, and the PSS is installed to provide a pure positive damping torque in this paper. The loads are modelled as composite ZIP and induction motor load models. The damping coefficient D of generator G3 is set to be -2.5 while it should be positive. It should be noted that if the damping coefficient D is set to zero, a negative damping can be excited when the gain of the PSS is set to be a wrong value in the test system. In this paper, the negative damping coefficient is helpful to excite the negative damping mode, and the similar setting is adopted in [7], [8]. A three-phase fault lasting for 0.1s is applied at bus 7 to initiate the transient responses. All simulations are run on the Power System Toolbox platform in the MATLAB environment and the sample time are 0.01s.

1) OBSERVATION OF $K5$

In general, a negative $K5$ will result in a negative damping torque. Then, we compute the $K5$ in the two-area case based on the equation in [4] and the $K5$ of each generator is presented in Table 1. It can be seen that the $K5$ is positive and AVR contributes positively to the oscillation in this case.

TABLE 1. Observation of $K5$ in each generator.

Generator	G1	G2	G3	G4
$K5$	0.054	0.049	0.051	0.053

2) PERFORMANCE WITHOUT MEASUREMENT NOISES

The proposed method is verified based on ideal ring-down signals, and the results are compared with the method developed in [7]. According to the implementation steps in section IV, the oscillation energy calculation is explained as follows.

Step 1: Obtain and pre-process the input signals. The active power deviations and speed deviations of all generators are collected as the input signals. Then, a detrend technique is conducted to remove linear trends in the signals.

Step 2: Modal analysis. The Eigen-analysis result shows that there are one inter-area mode and two local modes. Table 2 shows the frequencies (f) and damping ratios (d). It is clear that mode 1 and mode 3 are the poorly damped modes, and mode 1 is the inter-area mode, which involves more generators than local modes. Thus, mode 1 is selected as the dominant mode for analysis.

It should be noted that when applying the proposed method in real power systems, step 2 is done by implementing the

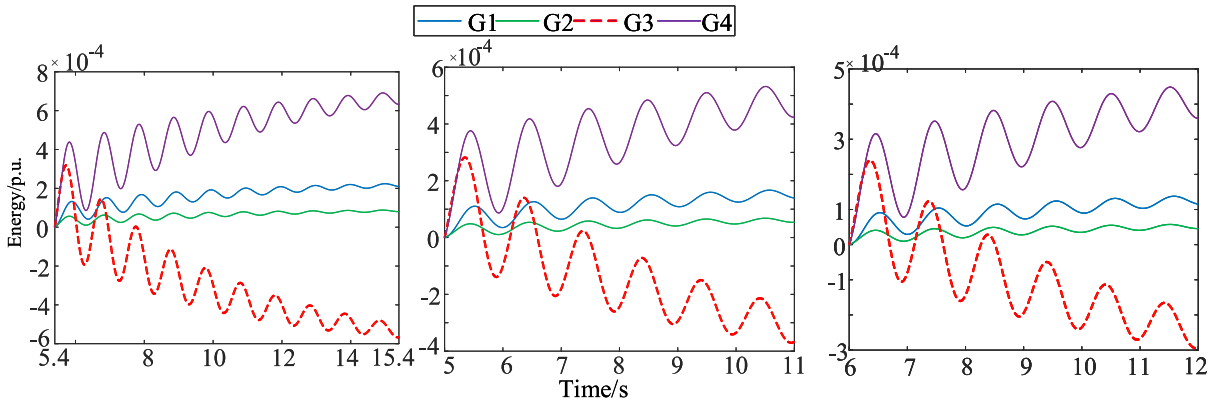

FIGURE 4. Oscillation energy calculated by proposed method in different time windows.

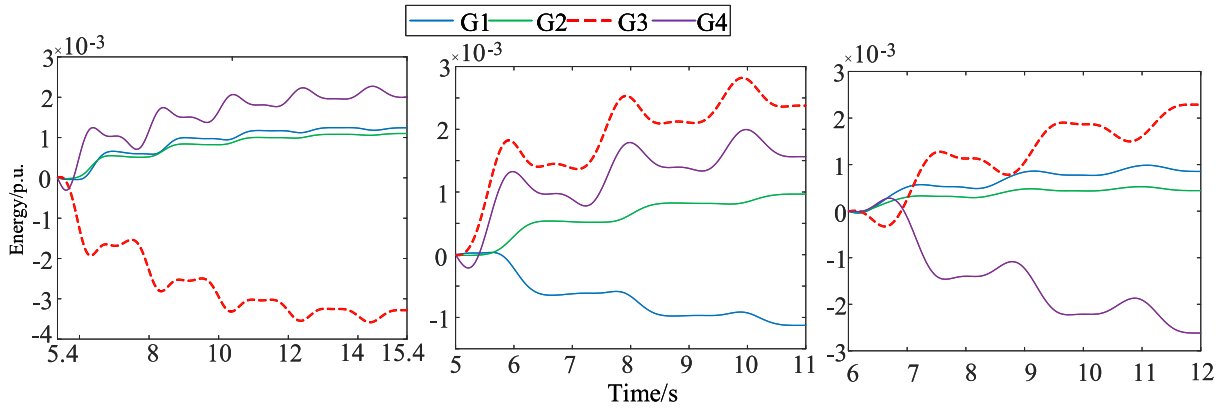

FIGURE 5. Oscillation energy calculated by method in [7] in different time windows.

TABLE 2. Frequencies and damping ratios based on Eigen-analysis.

Mode 1		Mode 2		Mode 3	
f/Hz	d/%	f/Hz	d/%	f/Hz	d/%
0.6201	2.45	1.1576	10.42	1.1751	1.24

PRCE method [22] since the model-based Eigen-analysis may lead to wrong results [23].

Step 3: Extract the oscillation component. Select the generator speed deviations $\Delta\omega_i$ $(i = 1, 2, 3, 4)$ and active power deviations ΔP_{ei} $(i = 1, 2, 3, 4)$ during 5s-20s as the inputs, and apply the PRCE method to obtain the oscillation parameters of each signal for mode 1. Based on the parameters estimated by PRCE, the oscillation component $\Delta P_{ei}|_{\lambda_1}$ and $\Delta\omega_i|_{\lambda_1}$ can be obtained by (15).

Step 4: Oscillation energy calculation. To verify the performance of the proposed method, the oscillation energy is computed with the sliding window technique [23]. The frequency of domain mode is 0.7231Hz, and the period is about 1.4s. Generally, in order to obtain the accurate oscillation information of inter-area oscillations, the length of the time window needs to be several times the period of the lowest frequency oscillation mode concerned. In this paper, the length of each time window is 10s, which includes several circles of the domain mode, and the time window is shifted by 1s each time. Fig. 4 and Fig. 5 show the oscillation energy in three different time windows using the proposed method and method in [7]. From Fig. 4, we can see that the oscillation energy of G3 for mode 1 decreases with time in different time windows, indicating that G3 has a negative damping contribution to the system. Thus, G3 is identified as the only generator contributing negative damping, which is consistent with the simulation setting. Meanwhile, the slopes of oscillation energy of every generator in different windows do not change much.

On the other hand, in Fig. 5, the oscillation energy of the same generator has a variation in different time windows, which cannot be used to determine negative damping generators. This variation exists because the input data contain multi-oscillation modes, but the method in [7] only works for single-mode oscillations.

3) PERFORMANCE IN NOISE CONDITION

In actual power systems, the measurement data usually include noises. To evaluate the robustness of the proposed

method against measurement noises, white Gaussian noises are added to the raw signals [22], [23]. The noise levels are represented by SNRs (signal-to-noise ratios), with the unit dB:

$$\mathrm{SNR} = 10\lg P_{signal}/P_{noise} \tag{22}$$

where P_{signal} and P_{noise} are the power of signal and noise, respectively. The SNR is set to be 20dB, which represents a high level of measurement noise.

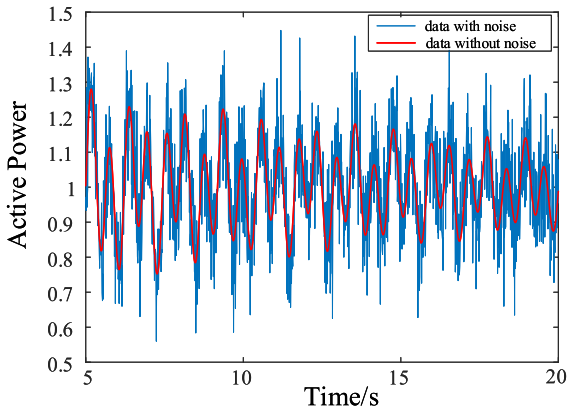

FIGURE 6. Calculated oscillation energy based on noise signal.

In this case, the SNR is set to be 20dB, which represents a high level of measurement noise. Fig. 6 shows the original active power signal and the signal with the noise of generator 4 when SNR = 20dB.

After obtaining the signal with noise, we conduct the procedure according to Fig. 3. The calculated oscillation energies of four generators in mode 1 are shown in Fig. 7. It is shown that the location result is consistent with the simulation settings. In addition, the calculated oscillation energies are represented by smooth curves, which show the robustness of the low-frequency oscillation analysis method used in Step 2. In this paper, the measurement noise are tackled by the following process. The raw measurement is first processed by a low-pass (LP) filter and the high frequency noises are extracted and removed. Then, the filtered data is processed by PRCE method to obtain smooth oscillation components. These methods are validated to be robust and can generate smooth oscillation components from raw measurements. The oscillation energies are finally computed based on these components without noises. Therefore, the proposed method can be applied to the actual system when the measurement data contain noises.

4) PERFORMANCE IN DIFFERENT LOAD LEVELS

The load conditions affect modal damping. In general, a light load makes the system more stable, and a heavy load may result in an unstable system. In this section, we evaluate the proposed method under different load conditions. Table 3 shows the damping ratio and frequency of mode 1 in different load conditions.

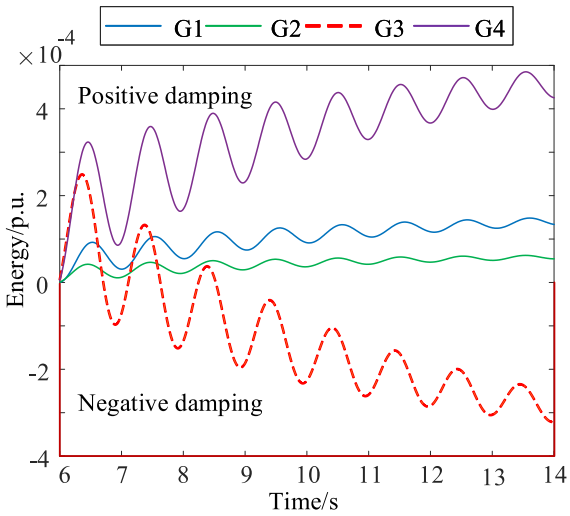

FIGURE 7. Calculated oscillation energy based on noise signal.

TABLE 3. Damping information under different load conditions.

Load/%	80	90	100	110	120
D/%	2.75	2.471	2.45	2.443	2.437
F/Hz	0.6205	0.6205	0.6201	0.6118	0.6117

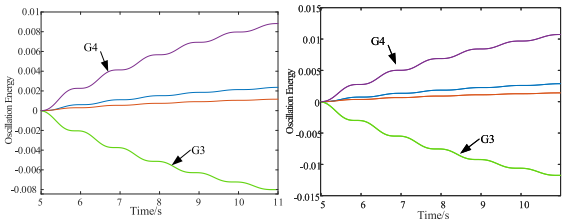

FIGURE 8. Oscillation energies in different load conditions.

Fig. 8 shows the oscillation energy in two load conditions. From this figure, we can see that the proposed method can accurately evaluate the damping effect under different load conditions.

5) IMPACT OF TIME DELAY

In real power systems, the delay of a signal feedback in a wide-area power system is usually in the order of 100ms. For ring-down oscillations, the length of time window to obtain the accurate information for inter-area oscillations is generally set to 5s-10s. Therefore, the 0.1s delay may not cause significant impact. In order to demonstrate it, a sliding time window method is adopted to estimate the damping ratio and frequency under different measurement periods, and the length of sliding time window is 1s.

Table 4 shows the estimated damping under different time windows. From the table we can see that the oscillation

TABLE 4. Damping ratios and frequencies based on different period measurements.

Time period/s	Damping ratio/%	Frequency/Hz
2-10	2.433	0.6118
3-11	2.464	0.6211
4-12	2.461	0.6211

analysis results are very close under different time periods. In addition, we have demonstrated that the proposed method can accurately locate the poorly damped generator in different time windows. Therefore, the proposed method is effective with the communication time delay.

B. 16-MACHINE SYSTEM

The proposed method is further tested on a 16-machine power system under different operating conditions. All 16 generators are represented by detailed synchronous machine models, and each generator is equipped with dc exciters with PSS, with the single line diagram referred in [24].

1) PERFORMANCE IN THE SINGLE NEGATIVE DAMPING GENERATOR SCENARIO

The damping coefficient D of generator G16 is set to be negative, which should be positive in normal condition. A three-phase fault lasting for 0.1s is applied at bus 27 to generate the time-domain simulation data.

The Eigen-analysis shows that there are four inter-area modes and eleven local modes in this system. Table 5 indicates that mode 2 is a poorly damped inter-area mode. In addition, the damping ratios of other inter-area modes are larger than 5%. Thus, mode 2 is selected as the dominant mode for oscillation energy analysis. The oscillation energy of all generators in mode 2 is shown in Fig. 9. It can be seen that G16 is the only generator with negative damping in mode 2. Thus, G16 is the generator with negative damping, which is consistent with the simulation settings.

TABLE 5. Frequencies and damping ratios in 16-machine system.

Mode 1		Mode 2		Mode 3		Mode 4	
f/Hz	d/%	f/Hz	d/%	f/Hz	d/%	f/Hz	d/%
0.3817	8.9	0.5161	1.37	0.6674	5.90	0.7902	8.37

In order to test the performance of the proposed method, the energy function developed in this paper is compared with the method proposed in [13]. In [13], authors used the OLS method to calculate the damping coefficients of each generator. The input signals for that method are decomposed active power deviation, decomposed speed deviation and power angle deviation of each generator. Fig. 10 shows the

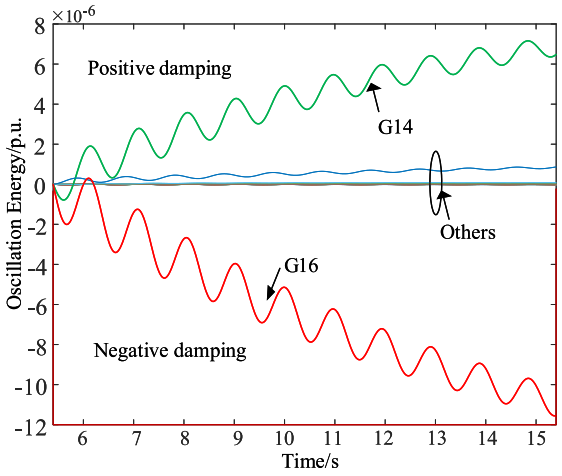

FIGURE 9. Oscillation energy of generators in mode 2.

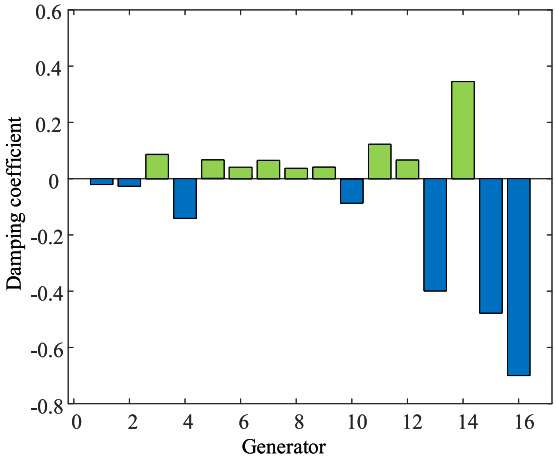

FIGURE 10. Damping coefficients with respect to mode 2.

calculated damping coefficients of all generators according to the method in [13] with respect to mode 2. From Fig. 10, there are 6 generators with negative damping coefficients, and some of the negative coefficients are close to each other, which is inconsistent with the simulation setting and would make it difficult to identify the generators with negative damping. However, based on the proposed method, generators contributing negative damping can be clearly identified, as shown in Fig. 9.

2) PERFORMANCE IN MULTI-GENERATORS WITH NEGATIVE DAMPING SCENARIO

To validate the performance of the proposed method for locating multi-generators with negative damping, the damping coefficient of G13 is also set to be negative, in addition to the wrong parameter of G16. According to the modal analysis results, there are two poorly damped oscillation modes in this case, inter-area modes 2 and 3. Thus, inter-area modes 2 and 3 are selected as the dominant modes for evaluating generator damping. To obtain the time-domain response, we conduct

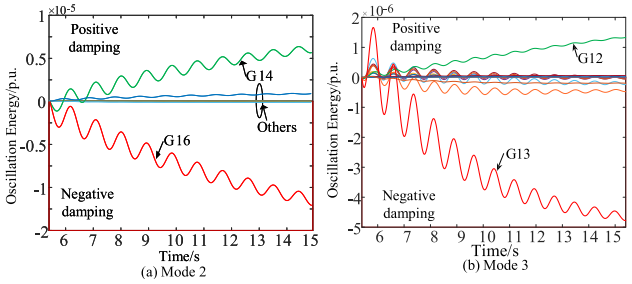

FIGURE 11. Oscillation energies in mode 2 and mode 3.

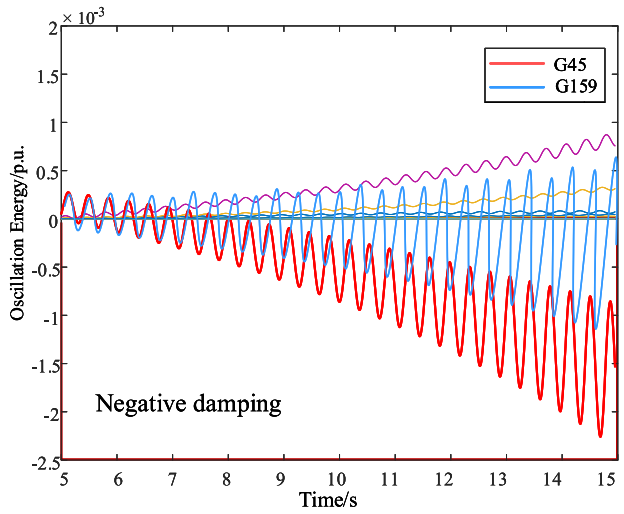

FIGURE 12. Oscillation energies in case ND6.

the same process as in section IV. According to the process in section IV, the oscillation components of $\Delta P_{ei}|_{\lambda_2}$ and $\Delta\omega_i|_{\lambda_2}$ are first reconstructed, then the oscillation energies all 16 generators are calculated by (20). Fig. 11 shows the corresponding oscillation energies in mode 2 and mode 3.

From Fig. 11 (a), we can see that the oscillation energy of G16 in mode 2 decreases with time. Therefore, generator 16 is identified as a generator contributing negative damping to mode 2. Similarly, from Fig. 11 (b), it is clear that generator 13 can be labelled as the generator with negative damping in mode 3. These observations are consistent with the simulation settings.

C. WECC 179-BUS SYSTEM

In order to further validate the proposed method, we apply the proposed method to the WECC 179-bus system provided in the test case library [25]. In this section, the natural oscillation case ND6 shown in test case library is adopted. This case contains two sources G45 and G159 and a single unstable local mode with 1.41Hz oscillation frequency. The dynamic simulation is implemented on PSS/E, and measurements from 5s to 15s is adopted. Fig. 12 shows the oscillation energies. It can be seen that G159 and G45 are identified with negative damping effect, which is consistent with the settings in this case. In [8], the DEF-based method locates two negative damping generators with measurements from 34s to 40s. However, according to the simulation, the system collapsed at 27s. Compared with the DEF method, the proposed method can correctly identify negative damping generators in a shorter time and help suppress the sustained oscillation.

VI. CONCLUSION

This paper analyzes the electric torque in multi-machine power systems and proposes a hybrid energy and mode decomposition-based generator damping evaluation approach for multi-machine power systems. The oscillation components for each oscillation mode are first extracted, and then the generator damping is estimated using a newly defined oscillation energy function. Based on the oscillation energy results in the concerned mode, generators with attenuated oscillation energies have a negative damping effect. The proposed method is not only purely measurement-based, but also robust against measurement noises. Simulation results in different test cases show that the proposed method is effective to evaluate generators damping in multi-machine power systems. In future work, the proposed method will be extended to estimate generators' damping effects using ambient signals, which can monitor power systems in a wider time range.

REFERENCES

[1] D. N. Kosterev, C. W. Taylor, and W. A. Mittelstadt, "Model validation for the august 10, 1996 WSCC system outage," *IEEE Trans. Power Syst.*, vol. 14, no. 3, pp. 967–979, Aug. 1999.

[2] D. Yang, B. Wang, G. Cai, Z. Chen, J. Ma, Z. Sun, and L. Wang, "Data-driven estimation of inertia for multiarea interconnected power systems using dynamic mode decomposition," *IEEE Trans. Ind. Informat.*, vol. 17, no. 4, pp. 2686–2695, Apr. 2021.

[3] B. Wang and K. Sun, "Formulation and characterization of power system electromechanical oscillations," *IEEE Trans. Power Syst.*, vol. 31, no. 6, pp. 5082–5093, Nov. 2016.

[4] P. Kundur, N. J. Balu, and M. G. Lauby, *ower System Stability and Control*, vol. 7. New York, NY, USA: McGraw-Hill, 1994.

[5] J. Zhang and H. Xu, "Online identification of power system equivalent inertia constant," *IEEE Trans. Ind. Electron.*, vol. 64, no. 10, pp. 8098–8107, Oct. 2017.

[6] X. Xu, W. Ju, B. Wang, and K. Sun, "Real-time damping estimation on nonlinear electromechanical oscillation," *IEEE Trans. Power Syst.*, early access, Dec. 2, 2020.

[7] L. Chen, Y. Min, and W. Hu, "An energy-based method for location of power system oscillation source," *IEEE Trans. Power Syst.*, vol. 28, no. 2, pp. 828–836, May 2013.

[8] S. Maslennikov, B. Wang, and E. Litvinov, "Dissipating energy flow method for locating the source of sustained oscillations," *Int. J. Electr. Power Energy Syst.*, vol. 88, pp. 55–62, Jun. 2017.

[9] B. Wang and K. Sun, "Location methods of oscillation sources in power systems: A survey," *J. Modern Power Syst. Clean Energy*, vol. 5, no. 2, pp. 151–159, Mar. 2017.

[10] R. Alden and A. Shaltout, "Analysis of damping and synchronizing torques—Part I—A general calculation method," *IEEE Trans. Power App. Syst.*, vol. PAS-98, no. 5, pp. 1696–1700, Sep. 1979.

[11] A. A. Shaltout and K. A. Abu Al-Feilat, "Damping and synchronizing torque computation in multimachine power systems," *IEEE Trans. Power Syst.*, vol. 7, no. 1, pp. 280–286, Feb. 1992.

[12] R. Jalayer and B.-T. Ooi, "Estimation of electromechanical modes of power systems by transfer function and eigenfunction analysis," *IEEE Trans. Power Syst.*, vol. 28, no. 1, pp. 181–189, Feb. 2013.

[13] Y. Li, Y. Huang, J. Liu, W. Yao, and J. Wen, "Power system oscillation source location based on damping torque analysis," *Power Syst. Protection Control*, vol. 43, no. 14, pp. 84–91, 2015.

[14] S. Feng, B. Zheng, P. Jiang, and J. Lei, "A two-level forced oscillations source location method based on phasor and energy analysis," *IEEE Access*, vol. 6, pp. 44318–44327, 2018.
[15] L. Chen, F. Xu, Y. Min, M. Wang, and W. Hu, "Transient energy dissipation of resistances and its effect on power system damping," *Int. J. Electr. Power Energy Syst.*, vol. 91, pp. 201–208, Oct. 2017.
[16] Y. Shu, S. Grid Corporation of China, X. Zhou, W. Li, C. Electric Power Research Institute, and C. Electric Power Research Institute, "Analysis of low frequency oscillation and source location in power systems," *CSEE J. Power Energy Syst.*, vol. 4, no. 1, pp. 58–66, Mar. 2018.
[17] L. Chen, Y. Min, X. Lu, X. Xu, Y. Li, Y. Zhang, and Q. Chen, "Online emergency control to suppress frequency oscillations based on damping evaluation using dissipation energy flow," *Int. J. Electr. Power Energy Syst.*, vol. 103, pp. 414–420, Dec. 2018.
[18] R. Xie and D. J. Trudnowski, "Tracking the damping contribution of a power system component under ambient conditions," *IEEE Trans. Power Syst.*, vol. 33, no. 1, pp. 1116–1117, Jan. 2018.
[19] H. Wang and W. Du, *Analysis and Damping Control of Power System Low-Frequency Oscillations*. New York, NY, USA: Springer, 2016.
[20] F. J. Swift and H. F. Wang, "The connection between modal analysis and electric torque analysis in studying the oscillation stability of multi-machine power systems," *Int. J. Electr. Power Energy Syst.*, vol. 19, no. 5, pp. 321–330, Jun. 1997.
[21] L. Peng, Y. Yixin, and S. Qiang, "Computation of electric torque coefficients in multi-machine power systems based on prony analysis," *Power Syst. Technol.-Beijing*, vol. 30, no. 10, p. 39, 2006.
[22] J. Xie and X. Wang, "Estimation of electromechanical modes under ambient condition through random decrement technique and PRCE algorithm," in *Proc. IEEE PES Asia–Pacific Power Energy Eng. Conf. (APPEEC)*, Oct. 2016, pp. 509–514.
[23] J. M. Seppanen, J. Turunen, M. Koivisto, N. Kishor, and L. C. Haarla, "Modal analysis of power systems through natural excitation technique," *IEEE Trans. Power Syst.*, vol. 29, no. 4, pp. 1642–1652, Jul. 2014.
[24] G. Rogers, *Power System Oscillations*. New York, NY, USA: Springer, 2012.
[25] S. Maslennikov, B. Wang, Q. Zhang, A. Ma, A. Luo, A. Sun, and E. Litvinov, "A test cases library for methods locating the sources of sustained oscillations," in *Proc. IEEE Power Energy Soc. Gen. Meeting (PESGM)*, Jul. 2016, pp. 1–5.

JIAN XIE (Graduate Student Member, IEEE) received the B.S. and M.S. degrees in electrical engineering from Southwest Jiaotong University, Chengdu, China, in 2015 and 2018, respectively. He is currently pursuing the Ph.D. degree with the Department of Electrical and Computer Engineering, University of Central Florida, Orlando, FL, USA. His research interests include power system stability and machine learning in power system resilience enhancement.

WEI SUN (Member, IEEE) received the Ph.D. degree from Iowa State University, Ames, IA, USA, in 2011. He is currently an Associate Professor with the Department of Electrical and Computer Engineering, University of Central Florida, Orlando, FL, USA. He is also the Director of the Siemens Digital Grid Laboratory. His research interests include power system restoration, self-healing smart grid, and cyber-physical system security and resilience.

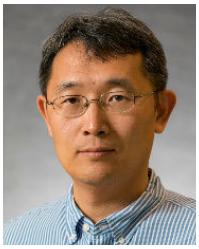

KAI SUN (Senior Member, IEEE) received the B.S. degree in automation and the Ph.D. degree in control science and engineering from Tsinghua University, Beijing, China, in 1999 and 2004, respectively. From 2007 to 2012, he was a Project Manager in grid operations and planning with the Electric Power Research Institute (EPRI), Palo Alto, CA, USA. He is currently an Associate Professor with the Department of Electrical Engineering and Computer Science, The University of Tennessee, Knoxville, USA. He is also an Associate Editor of IEEE TRANSACTIONS ON POWER SYSTEMS, IEEE TRANSACTIONS ON SMART GRID, IEEE ACCESS, and IEEE OPEN ACCESS JOURNAL OF POWER AND ENERGY.

XIAORU WANG (Senior Member, IEEE) received the B.S. and M.S. degrees from Chongqing University, Chongqing, China, in 1983 and 1988, respectively, and the Ph.D. degree from Southwest Jiaotong University, Chengdu, China, in 1998. Since 2002, she has been a Professor with the School of Electrical Engineering, Southwest Jiaotong University. Her current research interests include electric power systems protection and stability control, integrated renewable energy, and smart grid.